This manuscript has been authored by UT-Battelle, LLC under Contract No. DE-AC05-00OR22725 with the U.S. Department of Energy. The United States Government retains and the publisher, by accepting the article for publication, acknowledges that the United States Government retains a non-exclusive, paid-up, irrevocable, world-wide license to publish or reproduce the published form of this manuscript, or allow others to do so, for United States Government purposes. The Department of Energy will provide public access to these results of federally sponsored research in accordance with the DOE Public Access Plan(http://energy.gov/downloads/doe-public-access-plan).

The Behavior of Bilayer Leaflets in Asymmetric Model Membranes: Atomistic Simulation Studies

Jianhui Tian,[1] Jonathan Nickels,[2] John Katsaras,[2,3,] Xiaolin Cheng[1*]

1. Center for Molecular Biophysics, Oak Ridge National Laboratory, Oak Ridge, TN 37831
2. Joint Institute for Neutron Sciences, Oak Ridge National Laboratory, Oak Ridge, TN 37831
3. The Bredesen Center for Interdisciplinary Research and Graduate Education 444 Greve Hall, 821 Volunteer Blvd. Knoxville, TN 37996-3394
4. Neutron Sciences Directorate, Oak Ridge National Laboratory, Oak Ridge, TN 37831

* Corresponding author: Xiaolin Cheng, chengx@ornl.gov, phone number: 865-576-0850

Abstract

The spatial organization within lipid bilayers is an important feature for a range of biological processes. Leaflet compositional asymmetry and lateral lipid organization are just two of the ways in which membrane structure appears to be more complex than initially postulated by the fluid mosaic model. This raises the question of how the phase behavior in one bilayer leaflet may affect the apposing leaflet, and how one begins to construct asymmetric model systems to investigate these interleaflet interactions. Here we report of all-atom molecular dynamics simulations (a total of 4.1 μs) of symmetric and asymmetric bilayer systems composed of liquid-ordered (Lo) or liquid-disordered (Ld) leaflets, based on the nanodomain forming POPC/DSPC/cholesterol system. We begin by analyzing an asymmetric bilayer with leaflets derived from simulations of symmetric Lo and Ld bilayers. In this system, we observe that the properties of the Lo and Ld leaflets are similar to those of the Lo and Ld leaflets in corresponding symmetric systems. However, it is not obvious that mixing the equilibrium structures of their symmetric counterparts is the most appropriate way to construct asymmetric bilayers, nor that these structures will manifest interleaflet couplings that lead to domain registry/anti-registry. We therefore constructed and simulated four additional asymmetric bilayer systems by systematically adding or removing lipids in the Ld leaflet, to mimic potential density fluctuations. We find that the number of lipids in the Ld leaflet affects its own properties, as well as those of the apposing Lo leaflet. Collectively, the simulations reveal the presence of weak acyl chain interdigitation across bilayer leaflets, suggesting that interdigitation alone does not contribute significantly to the interleaflet coupling in non-phase-separated bilayers of this chemical composition. However, the properties of both

leaflets appear to be sensitive to changes in in-plane lipid packing, possibly providing a mechanism for interleaflet coupling by modulating local density and/or curvature fluctuations.

Introduction

The plasma membrane (PM) separates the interior of a cell from its outside environment and acts as a functional interface, where biochemical processes can take place. The molecular organization of the PM is now thought to be more complex than originally proposed by the Singer and Nicolson fluid mosaic model of the PM[1]. It is now well known that compositional differences between bilayer leaflets[2-3] and lateral heterogeneity[4] are vital to a number of biochemical processes. For instance, lateral organization is believed to play a role in signal transduction[5], apoptosis[6], cell adhesion and migration[7], cell recognition[8], synaptic transmission[9], cytoskeletal organization[10] and protein sorting [11-12]. Bilayer compositional asymmetry, on the other hand, has been suggested to be involved in signaling apoptosis[13-16], thrombosis[17-18], phagocytosis[13, 19-21], and as an indicator of tumorigenic cells[22-23].

The interplay of these two organizational principles is an emerging question in the study of membrane biochemistry, biophysics and physical chemistry. In the case of mammalian PMs, the chemical compositions of the two leaflets are very different, [24] with the extracellular leaflet containing a mixture of sphingolipids, unsaturated glycerophospholipids, and cholesterol. When using a simplified mixture of these lipids, their tendency is to phase separate into coexisting fluid phases. [25] The phases primarily differ from each other in that they possess different hydrocarbon chain order and translational diffusion rates.[26] In contrast, the cytoplasmic leaflet is mainly composed of unsaturated phosphatidylcholine, phosphatidylethanolamine, phosphatidylserine and cholesterol, which do not phase separate in simplified membrane models.[27] Nevertheless,

it has been shown in model systems that the presence of domains in the membrane's outer leaflet can induce domain formation in its inner leaflet.[28] This highlights the possibility that these two organizational principles are somehow interconnected, a notion vital to bilayer lateral structural organization and how information is communicated across the membrane.

There is much debate as to the physical mechanisms involved in domain formation and interleaflet coupling[29-31]. In natural PMs, lateral organization and interleaflet coupling are likely to be affected, or controlled, by the presence of bilayer-spanning proteins, which "connect" the bilayer's two leaflets. In addition to other features such as rapid lipid turnover and cytoskeletal interactions[32], it is clear that the PM's organization is maintained through active processes. However, observations in protein-free model systems suggest that lateral organization and interleaflet coupling can also occur due to the intrinsic properties of the lipids making up the bilayer[33-34]. Local curvature and density coupling have been proposed in driving raft formation across bilayer leaflets[35], while simulation studies have shown that membrane curvature and domain anti-registration are induced by domain-height mismatch.[36] In a recent study of interleaflet coupling mechanisms, including electrostatic coupling, cholesterol flip-flop and dynamic chain interdigitation, May[31] concluded that dynamic chain interdigitation is a major factor for interleaflet coupling, a notion also supported by Chiantia et al.'s work on asymmetric vesicles[33]. However, midplane surface tension[37], leaflet spontaneous curvature[38], monolayer height fluctuations[39] and the bilayer's bending rigidity have also been proposed as important mechanisms for leaflet coupling. When combined with the local

compositional differences found in lipid domains and the line tension associated with the domain interface[40-41], the delicate interplay of lateral organization and bilayer asymmetry comes to the forefront.

In the current study, we focus on the development of a series of computational models designed to interrogate the above-mentioned interleaflet effects. All-atom molecular dynamics (MD) simulations provide a full description of the microscopic interactions taking place in a lipid bilayer system, and make it possible to probe the physical interactions that can lead to macroscopic coupling phenomena. We have studied symmetric and asymmetric bilayer systems composed of laterally homogeneous leaflets in the liquid ordered (Lo) and liquid disordered (Ld) phases in lipid mixtures contain a high melting temperature (T_m) lipid (1,2-distearoyl-*sn*-glycero-3-phosphocholine, DSPC), a low T_m lipid (1-palmitoyl-2-oleoyl-*sn*-glycero-3- phosphocholine, POPC) and cholesterol (CHL), reflecting the composition of an experimentally studied system[42-44], where in-register[43] nanoscopic[42, 44] domains have been reported. By constructing asymmetric systems of the two coexisting phases and comparing to their symmetric counterparts, we seek to identify molecular mechanisms that may lead to the domain registry observed experimentally[43]. The simulations show that the structural and dynamical properties of individual bilayer leaflets, such as area per lipid, lipid density profiles, acyl chain order parameters and lipid lateral diffusion, are not influenced by the different phase apposing leaflets. In fact, the two leaflets behave as a single unit, interacting with each other through the bilayer midplane. We then constructed and simulated four additional asymmetric bilayer systems, systematically increasing or

decreasing the number of lipids in the Ld leaflet. The effects of the change in lipid population in these additional simulations highlight trends in the different physical properties, and interleaflet couplings, which are sensitive to in-plane lipid packing, implying that local density fluctuations can be coupled with membrane tension to influence interleaflet coupling.

Methods

A total of seven non-phase-separated Lo or Ld phase lipid bilayer systems were studied, namely: symmetric Lo, symmetric Ld, and five asymmetric Lo/Ld systems. Both Lo and Ld phases are composed of the high T_m lipid 1,2-distearoyl-*sn*-glycero-3-phosphocholine (DSPC), the low T_m lipid 1-palmitoyl-2-oleoyl-*sn*-glycero-3-phosphocholine (POPC), and cholesterol (CHL). The compositions are summarized in Table 1, with the Lo phase containing DSPC:POPC:CHL in a ratio of 0.49:026:0.25, and the Ld phase in a ratio of 0.09:0.79:0.12, consistent with experimental studies[42-44]. The two symmetric Lo and Ld bilayer systems, denoted as LoLo and LdLd, respectively, were built using the CHARMM-GUI web server.[45] The numbers of lipids and water molecules for both systems are listed in Table 1.

When constructing asymmetric bilayers, it is important that both bilayer leaflets contain the correct number of lipids so that the surface tension within each leaflet is zero (i.e., a tensionless bilayer). Following the approach of Perlmutter et al,[36] we first built an asymmetric Lo/Ld system based on simulations of symmetric Lo and Ld bilayers. With the number of lipids fixed at 400 in the Lo leaflet, the requisite number of lipids in the Ld

leaflet was calculated from the area per lipid (APL) ratio between the LoLo and LdLd systems. If the phase behavior in the two leaflets is not coupled, the Lo and Ld leaflets in the asymmetric bilayer should have the same lateral area, and the bilayer is thus tensionless (denoted as LoLd(0)). However, it is not obvious that this assumption is valid. To investigate the possibility of interleaflet coupling effects, we built four additional asymmetric LoLd bilayers in which the number of Ld lipids was systematically varied by adding/removing 5 or 10 lipids. These bilayers are referred to as LoLd(0), LoLd(-5), LoLd(5), LoLd(-10), and LoLd(10) (Table 1).

Simulations were carried out using the GROMACS 5.0.1 program.[46] The CHARMM c36 force field[47] was used for the lipids, and the TIP3P[48] model for water. All systems were simulated under constant pressure (1 bar) and constant temperature (303 K) (NPT) with periodic boundary conditions.[47] The Nose-Hoover thermostat was used for temperature control with a 1.0 ps coupling constant,[49-50] and the Parrinello-Rahman extended ensemble coupling was used for pressure control with a coupling constant of 5.0 ps.[51] Pressure coupling was applied semi-isotropically, with the z dimension (i.e., perpendicular to the plane of the bilayer) allowed to fluctuate independently of the x and y dimensions. Long-range electrostatic interactions were treated using the particle-mesh Ewald method.[52] The van der Waals interactions were treated using a switching function to reduce the force to zero, from 0.8 to 1.2 nm, according to Piggot et al.'s work.[53] All bond interactions involving hydrogen atoms were constrained using SETTLE[54] and LINCS[55] to allow for a 2-fs integration time step. The LoLo, LdLd and LoLd(0) systems were each simulated for 700 ns, while the LoLd(-10), LoLd(-5), LoLd(5) and LoLd(10)

systems were each simulated for 500 ns. A total of 4.1 μs of simulations were performed and analysis was done for each of the trajectories – excluding the first 100 ns, unless otherwise stated.

Table 1. Detailed compositions of the bilayers studied.

System (two leaflets)	No. DSPC	No. POPC	No. CHL	No. Atoms	Time (ns)
LoLo	49	26	25	43847	700
	49	26	25		
LdLd	9	79	12	47095	700
	9	79	12		
LoLd(0)	196	104	100	164786	700
	22	240	33		
LoLd(-5)	196	104	100	164116	500
	22	235	33		
LoLd(5)	196	104	100	165620	500
	24	243	35		
LoLd(-10)	196	104	100	163462	500
	24	228	33		
LoLd(10)	196	104	100	166188	500
	28	243	35		

Interfacial (surface) tension is an important characteristic of a lipid bilayer as it determines its rigidity and stability, and is thus directly relevant for interpreting the various physical phenomena taking place in the lipid bilayer. The surface tension (γ) in each bilayer leaflet may not always be zero, as it can be compensated by membrane deformations. However, for an idealized (e.g., without undulation or spontaneous curvature) planar and laterally homogeneous lipid bilayer, γ each bilayer leaflet is expected to be zero. As a result, the surface tension, can in principle, be used as a guide for assembling asymmetric bilayers. γ can be calculated using the relationship $\gamma = -\int_0^h \pi(z)dz$, where $\pi(z)$ is the lateral pressure of the bilayer along the bilayer normal z,

and h is the bilayer thickness. Given the interaction forces and velocities of individual atoms in the system, the lateral pressure is calculated according to $\pi(z) = \frac{1}{2}\left(\overline{\sigma_{xx}(z)} + \overline{\sigma_{yy}(z)}\right) - \overline{\sigma_{zz}(z)}$, where σ_{xx}, σ_{yy}, and σ_{zz} are the components of the pressure tensor. We calculated the lateral pressure profiles for the symmetric LoLo and LdLd systems using Vanegas et al.'s customized GROMACS code,[56] with the results for simulation times of 100 ns , 300 ns and 500 ns shown in Figure 1. The lateral pressure profile of the LdLd system converged at 300 ns simulations, while the LoLo system converged at 500 ns. At 500 ns, the LdLd lateral pressure profile shows three peaks for each leaflet. They are associated with the lipid head group-water interface, the acyl chain hydrophobic region, and the bilayer midplane, respectively. Overall, the LdLd lateral pressure profile looks reasonably symmetric, and the integral of $\pi(z)$ for each leaflet is approximately zero (-0.8 dyn/cm), indicating that the leaflets are tensionless. At 500 ns, the LoLo lateral pressure profile also shows three peaks for each leaflet. Although a little noisier and not as symmetric as the LdLd system, $\pi(z)$ for each Lo leaflet also integrates to approximately zero (0.9 dyn/cm).

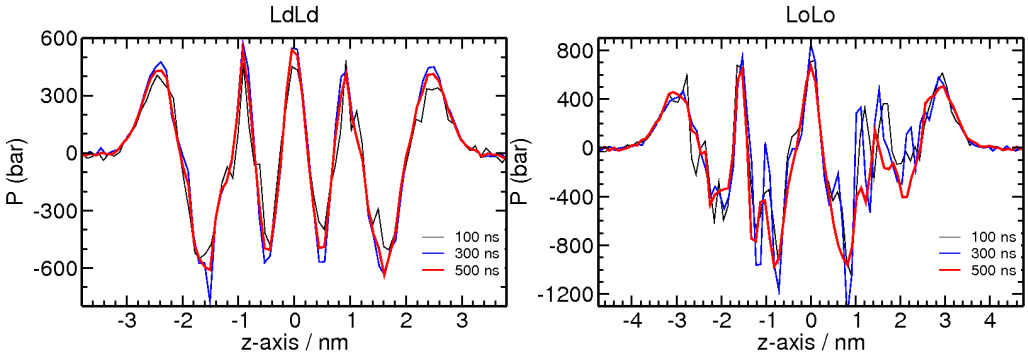

Figure 1. Lateral pressure profiles for symmetric LdLd and LoLo bilayers. Integration of the lateral pressure in individual Ld leaflets at 100, 300 and 500 ns leads to $\pi(z)$ of -5.6, -

1.2 and -0.8 dyn/cm, respectively. In the case of individual Lo leaflets at 100, 300, and 500 ns, $\pi(z)$ is -53, -10, and 0.9 dyn/cm, respectively.

Results

Asymmetric Bilayers Generated from Equilibrated Symmetric Bilayer Leaflets

The most straightforward method for assembling an asymmetric bilayer is to combine two different phase equilibrated leaflets, i.e., Ld and Lo. However, this may not appropriately reflect an equilibrated asymmetric bilayer. The challenge in building accurate asymmetric bilayers lies in understanding how they differ from symmetric bilayers. An asymmetric LoLd bilayer can be built by adjusting the number of lipids in the individual leaflets by using their respective lateral pressure profiles, essentially ensuring zero surface tension within each leaflet. However, this calculation is computationally very expensive (Figure 1). We thus took the structures of pre-equilibrated symmetric LoLo and LdLd bilayers to construct asymmetric bilayers. We chose the number of lipids in each Lo or Ld leaflet so that both leaflets would have the same surface area – denoted as LoLd(0). For subsequent comparisons, we also built and simulated four additional asymmetric LoLd systems with different numbers of lipids in the Ld leaflet to account for any possible interleaflet coupling effects (LoLd(-10), LoLd(-5), LoLd(+5), LoLd(+10)). We first compare the results of the LoLd(0) system to those from symmetric LoLo and LdLd bilayers. We then went on to compare the LoLd(0) system to the other four asymmetric systems.

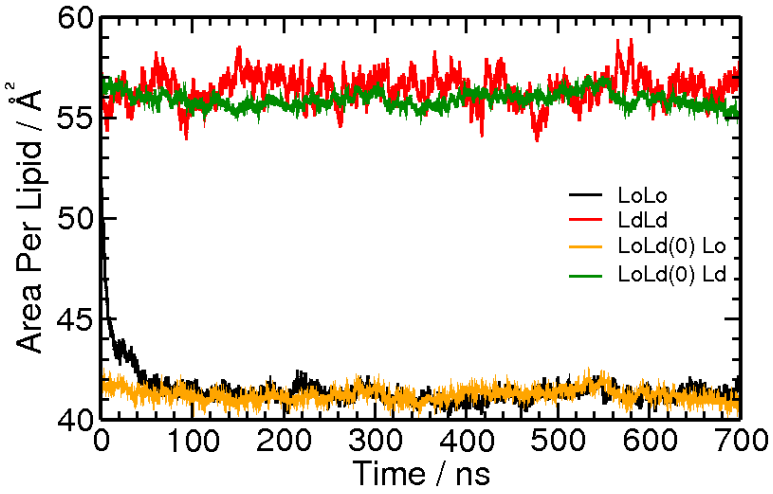

Figure 2. Time trajectories of APL for individual bilayer leaflets, namely LoLo (black), LdLd (red) and LoLd(0) (yellow and green). The yellow and green lines represent, respectively, the Lo and Ld leaflets in LoLd(0) asymmetric bilayers.

Area per lipid (APL) The equilibrated lateral structures of LoLo, LdLd and LoLd(0) bilayers were analyzed by calculating APL as a function of time (Figure 2). For the asymmetric LoLd(0) system, APLs for the Lo and Ld leaflets were calculated separately and compared to the corresponding values from the symmetric systems. As shown in Figure 2, a sharp decrease in APL is observed at the beginning of the symmetric LoLo simulation – likely due, initially, to lipids being loosely packed. The APLs for all three systems plateaued after ~100 ns. When calculating APLs we omitted the first 100 ns of simulation time. This was done for all subsequent analyses, unless noted. The computed APL is 56.5 ± 0.7 $Å^2$ for the symmetric Ld bilayer, and 41.3 ± 0.3 $Å^2$ for the symmetric Lo bilayer. Not surprisingly, lipids in the Lo phase are significantly more densely packed than those in the Ld phase. The APLs of the asymmetric LoLd(0) bilayer are 41.2 ± 0.3

$Å^2$ for the Lo leaflet and 55.9 ± 0.4 $Å^2$ for the Ld leaflet, in good agreement with values from corresponding symmetric Lo and Ld bilayers, respectively.

While APLs for these systems have not been experimentally determined, the related property of bilayer thickness has been measured by neutron scattering experiments.[43] We calculate bilayer thickness for the LoLo and LdLd systems to be 53.0 ± 0.9 Å and 44.2 ± 0.8 Å, respectively, and in good agreement with small angle neutron scattering (SANS) data (53.1 ± 1.0 Å for LoLo and 43.9 ± 1.4 Å for LdLd).[43] For the asymmetric LoLd system, the bilayer thickness is 49.1 ± 0.9 Å, a value reflecting the average of the symmetric LoLo and LdLd systems (48.6 ± 1.7 Å). Both APL and bilayer thickness results suggest that the phase asymmetry across the two leaflets has little effect on the in-plane lipid packing, and neither monolayer APL nor bilayer thickness is influenced by the apposing leaflet in laterally homogeneous bilayers.

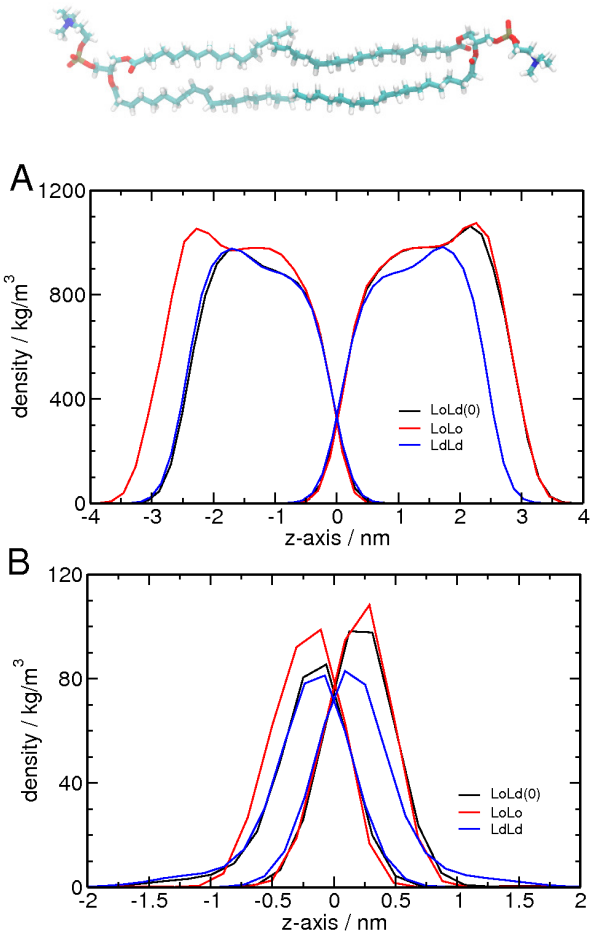

Figure 3. Lipid mass density profiles for lipids (A) and methyl carbons (B) in individual LoLo (red line), LdLd (blue line) and LoLd(0) (black line) bilayer leaflets.

Interdigitation The mass density profiles of lipids, as well as the methyl carbons for each leaflet were calculated and the results are shown in Figure 3. Lipid density profiles of the LdLd and LoLo systems are symmetric, with peak values of ~980 kg/m^3 and ~1070 kg/m^3, respectively. The LoLd(0) system exhibits an asymmetric density profile, with the two halves closely matching those of their respective symmetric leaflets, suggesting that the density profile of each leaflet in the asymmetric LoLd(0) system is not influenced by its neighbor. It is also interesting to note that the acyl chain density profiles

for all leaflets span the midplane, overlapping each other. The degree of overlap is the same for the three systems, approximately 2% of the total lipid density, a value similar to that reported by Capponi et al.[57] This is not unexpected as all three lipid bilayers contain DSPC and POPC, albeit in different ratios. The same degree of lipid tail mixing seen in all three systems also indicates that the strength of interdigitation does not appear to depend on the phase properties of the leaflets, but most likely on the length and chemical properties of their acyl chains.[58] In summary, the density profiles suggest weak acyl chain interdigitation for all three bilayers, but this weak interdigitation is unlikely to contribute to the interleaflet coupling, as evidenced by the fact that the density profiles of the individual bilayer leaflets are not influenced by their apposing leaflets.

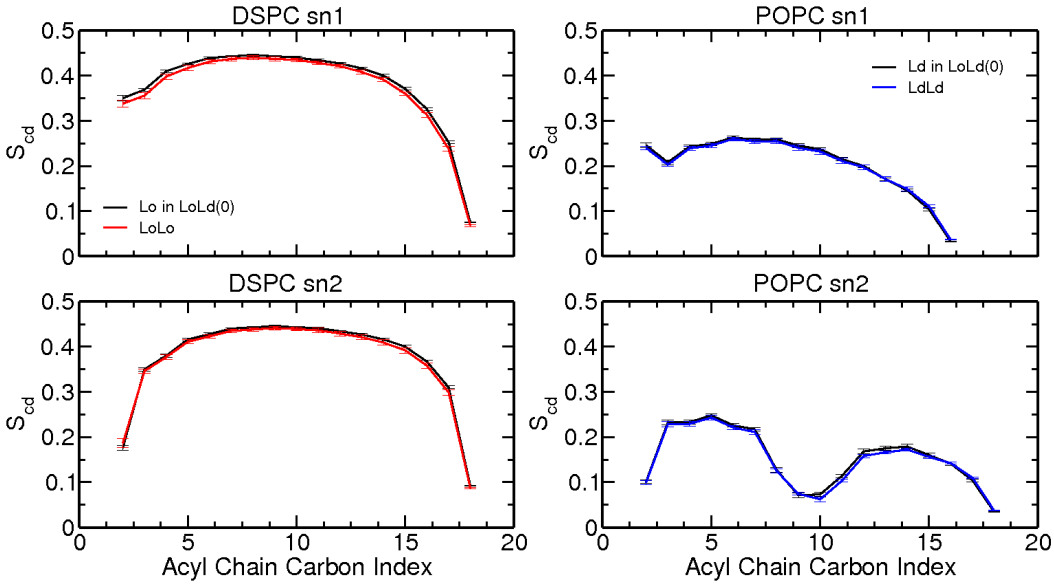

Figure 4. Acyl chain order parameters for DSPC in the Lo leaflet and POPC in the Ld leaflet. Order parameters for both sn-1 and sn-2 acyl chains in DSPC or POPC were calculated. Black, red and blue lines represent LoLd(0), LoLo and LdLd bilayers, respectively.

Order parameters Lipids in a fluid bilayer are highly dynamic. Lipid orientational mobility contributes significantly to the system's entropy, and is thus thought to be an essential consideration in the phase behavior of lipid bilayers. The deuterium order parameter is a convenient metric of these motions, a metric describing the orientational mobility of the C-D bond. It can be defined as $S = \langle\frac{3cos^2\theta-1}{2}\rangle$, where θ is the (time dependent) angle between the C-D bond vector and a reference axis. *S* for DSPC in the Lo leaflet and POPC in the Ld leaflet were calculated and are shown in Figure 4. As can be seen, *S* for the LoLd(0) asymmetric bilayer is similar to those in the corresponding symmetric Lo and Ld bilayers. This again suggests that the order parameters of the individual leaflets are not influenced by their apposing bilayer leaflets. This result differs from Perlmutter et al. who found that leaflet coupling led to ~10% change in the order parameters of lipids located across the center of an Lo domain in the apposing leaflet.[36] We propose two possible reasons for this discrepancy. First, our study used all atom force fields[47], while Perlmutter et al. used coarse grained Martini force fields[59]. Second, the two leaflets in our asymmetric bilayers contain lipids with similar acyl chain length, while those in the Perlmutter et al. study were composed of lipids with very different acyl chain length. The difference in acyl chain length has been shown to lead to stronger acyl chain interdigitation across the two leaflets[33], while differences in the interleaflet coupling, due to the use of different force fields, requires further investigation.

Table 2. Diffusion coefficients, in 10^{-7} cm^2/s, of DSPC and POPC in LoLo, LdLd, and LoLd(0) bilayers.

	LdLd	Ld in LoLd(0)	LoLo	Lo in LoLd(0)
DSPC	1.48±0.20	1.61±0.28	0.035±0.009	0.040±0.009
POPC	1.86±0.23	1.78±0.28	0.034±0.012	0.035±0.012

Lateral diffusion Lateral lipid diffusion has been suggested to be influenced by interleaflet coupling.[33] The self-diffusion coefficient *D* was estimated from simulations by evaluating the slope of the averaged mean square displacement (MSD) of the center of mass of individual lipids as a function of time. We removed the center of mass displacement for each monolayer in the manner used by Klauda et al[60], in order to eliminate finite size effects during simulation. Results for the LdLd, LoLo and LoLd(0) systems are listed in Table 2. The DSPC and POPC lipids in the Ld phase have comparable diffusion coefficients, with POPC (1.86±0.23 $\times 10^{-7}$ cm^2/s) diffusing slightly faster than DSPC (1.48±0.20 $\times 10^{-7}$ cm^2/s) – likely due to the unsaturated acyl chain in POPC disrupting local packing, and the preferential interaction of DSPC with cholesterol. It has previously been shown that both the degree of saturation/unsaturation of lipid acyl chains and lipid packing can affect lipid diffusion.[61-62] Compared to those in the Ld phase, DSPC and POPC in the Lo phase diffuse about 50 times slower. The most significant motions of these lipids in the Lo phase appear to be local rattling fluctuations that are highly correlated with their surrounding lipids. The diffusion coefficients calculated for DSPC and POPC in the Ld phase are comparable to experimental values,[61, 63-64] while the diffusion of DSPC and POPC in the Lo phase is about one order of magnitude slower than what was determined by experiment.[61, 63-64] Similar results have been reported for 1,2-dipalmitoyl-sn-glycero-3-phosphocholine (DPPC) with the CHARMM c36 force field.[65] However, the slow lipid diffusion in the Lo phase makes it difficult to confidently assess, within our simulation time scales, how lipid diffusion in

individual leaflets may be influenced by cross-layer coupling. Hence, we have focused our comparisons solely on the lateral diffusion in the Ld phase. It is evident that the time trajectories of DSPC and POPC MSDs in the Ld phase of asymmetric LoLd(0) bilayers (Supporting Information) coincide well with those of the LdLd symmetric system, suggesting that lipid diffusion in the Ld leaflet is not influenced by the apposing Lo leaflet in the case of the DSPC/POPC/CHL system.

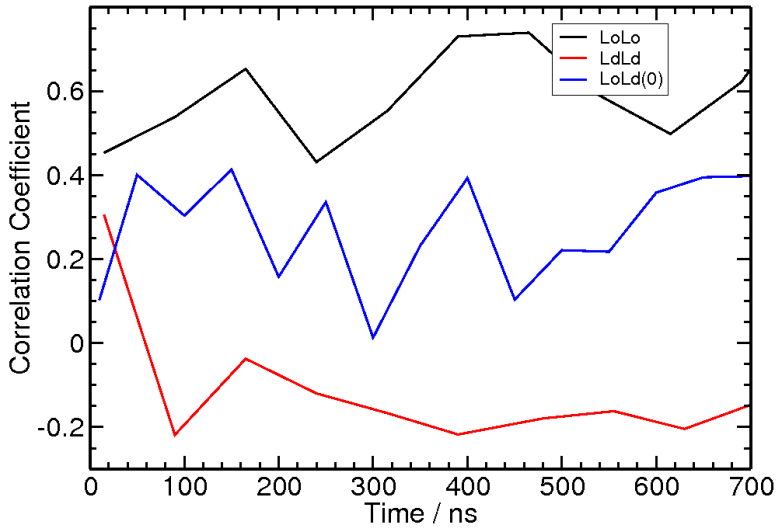

Figure 5. Lipid HGPCs as a function of time for LoLo (black line), LdLd (red line) and LoLd(0) (blue line) bilayers.

Lipid head group position correlation (HGPC) across leaflets Using continuum elasticity theory, Galimzyanov et al. showed that interleaflet coupling (domain registration) is driven by membrane deformations,[66] and that the bilayer's two leaflets interact with each other through the bilayer midplane. To quantify this interaction, we analyzed the correlated fluctuations of the lipid head groups across the leaflets (z-position). First, each leaflet was divided into a 6.5 Å × 6.5 Å grid, and z-positions were

calculated for all the cholines in the grid. Then the fluctuations of individual lipid head group positions were calculated with respect to the grid average positions. Finally, the Pearson correlation coefficient was calculated for the positional fluctuations of the two apposing lipid head groups.

HGPCs as a function of time for the three lipid bilayers are shown in Figure 5. The symmetric LoLo bilayer shows the strongest positional correlation (i.e., strongest midplane interaction), the symmetric LdLd bilayer shows the weakest correlation, and the asymmetric LoLd(0) system is in between the other two. This implies that the LoLo and LdLd bilayers have, respectively, the strongest and weakest midplane interactions. At the macroscopic scale, the Lo leaflet is more rigid, and therefore harder to compress than the Ld leaflet. The HGPC results are thus consistent with this prediction, that the two leaflets interact with each other through the bilayer midplane as a single unit. These differential bilayer midplane interactions further suggest that interleaflet tension differs in all three bilayers. Membrane interleaflet tension can drive domain formation[39] and has been proposed as a factor in domain interleaflet coupling,[67] since it can modulate domain height as well as the height mismatch across the asymmetric leaflets. Previous theory and simulations have shown that the domain height mismatch leads to domain anti-registration in asymmetric phase separated lipid bilayers,[36] in the gel domains of solid-supported bilayers[68] – this is in sharp contrast to what we observed experimentally in DSPC/POPC/CHL ternary mixtures.[43]

Comparison of individual bilayer leaflets in LoLo, LdLd and LoLd(0) systems suggests a lack of coupling in asymmetric, non-phase separated lipid bilayers of POPC/DSPC/CHL. The APLs of the Lo and Ld leaflets in the asymmetric bilayer are the same as those seen in the corresponding symmetric Lo and Ld bilayers. The deuterium order parameters for DSPC in the Lo leaflet and for POPC in the Ld leaflet of the asymmetric bilayer are also, within error , found to be the same as those in the corresponding symmetric bilayers. Furthermore, all three bilayers show a 2% acyl chain density overlap between their two leaflets, indicating some degree of lipid chain interdigitation. However, this weak interdigitation does not seem to couple the phase and physical properties of the two leaflets. Finally, lateral lipid self-diffusion in the Ld leaflet of the asymmetric system is indistinguishable from that in the symmetric LdLd system, while lipid diffusion in the Lo leaflet is too slow to draw any useful conclusions. A similar lack of interleaflet coupling has been reported by Bhide et al. on simulations of binary lipid mixture asymmetric bilayers.[69] These results demonstrate what we can learn through the approach of building asymmetric bilayers from pre-equilibrated symmetric leaflets, especially those that are laterally homogeneous.

Assembly of Asymmetric Bilayers by Adjusting Lipid Packing

We next analyzed four additional asymmetric bilayers that were constructed with differing numbers of lipids in the Ld leaflet to better reflect differences in lipid packing that may emerge due to bilayer asymmetry. These asymmetric bilayers have an Ld leaflet, whose number of lipids were systematically changed by adding or removing 5/10 lipids. They are denoted as LoLd(-10), LoLd(-5), LoLd(5) and LoLd(10). Using these

bilayers we wish to study how one bilayer leaflet compensates for short term fluctuations in the local lipid density taking place in the apposing leaflet.

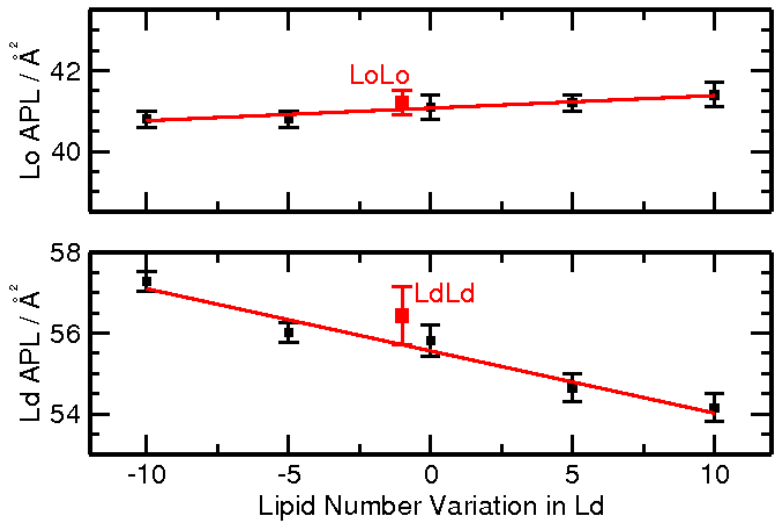

Figure 6. APLs of the Lo and Ld leaflets in LoLd(0), LoLd(-5), LoLd(5), LoLd(-10) and LoLd(10) bilayers, compared to symmetric LoLo and LdLd bilayers. The lines are the least squares fit to the data.

Area per lipid (APL) Changing the number of lipid molecules in the Ld leaflet of asymmetric bilayers affects lipid packing, as well as the packing of the apposing leaflet. Figure 6 shows the APLs for the Lo and Ld leaflets as a function of the change in the number of lipids in the different asymmetric bilayers, compared to the two symmetric systems. Increasing the number of lipids in the Ld leaflet causes the APL of the Ld leaflet to linearly decrease, while the APL of the apposing Lo leaflet shows an inverse behavior. This result implies an apparent coupling between the two leaflets – APL response is dictated by lateral compressibility. We fit the data using a linear least squares approach (Figure 6), and found that the decreasing slope for the Ld leaflet is five times that of the

increasing slope for the Lo leaflet, suggesting that the Ld leaflet is roughly five times more compressible (extensible) than the opposing Lo leaflet. Considering the area compressibility modulus K_A can be related to the bending modulus K_c through the relationship $K_A=24K_c/(2D_c)^2$, the above estimate is consistent with the bending moduli previously determined by experiment and simulation.[43]

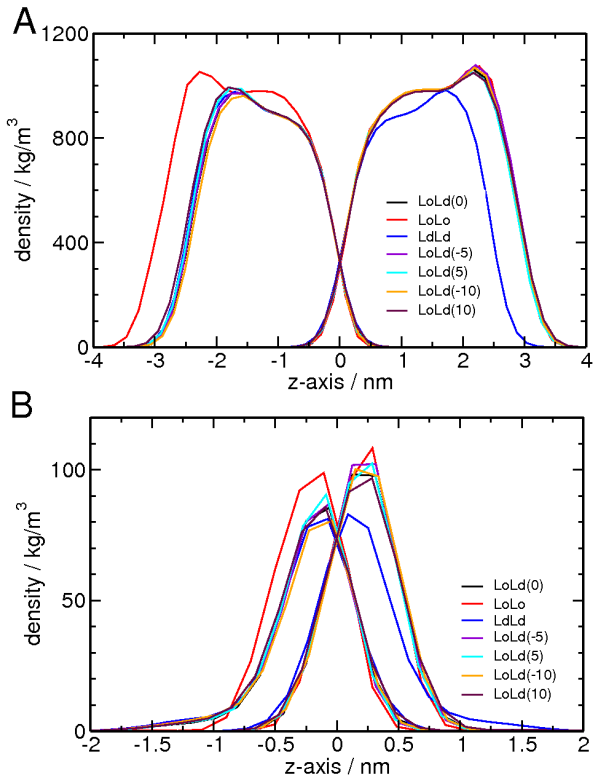

Figure 7. Lipid density profiles for lipids (A) and methyl carbons (B) for each leaflet in LoLo, LdLd, LoLd(0), LoLd(-5), LoLd(5), LoLd(-10) and LoLd(10) bilayers.

Interdigitation As shown in Figure 7, the lipid density profiles of the Lo and Ld leaflets in the four other asymmetric systems still resemble those of the corresponding Lo and Ld leaflets making up the symmetric bilayers. The degree of overlap between the two leaflets (Figure 7b) is consistently ~2% of the total lipid density for all systems. This result

suggests that the degree of acyl chain interdigitation between the two leaflets is unaffected by the induced APL changes taking place in the different asymmetric bilayers.

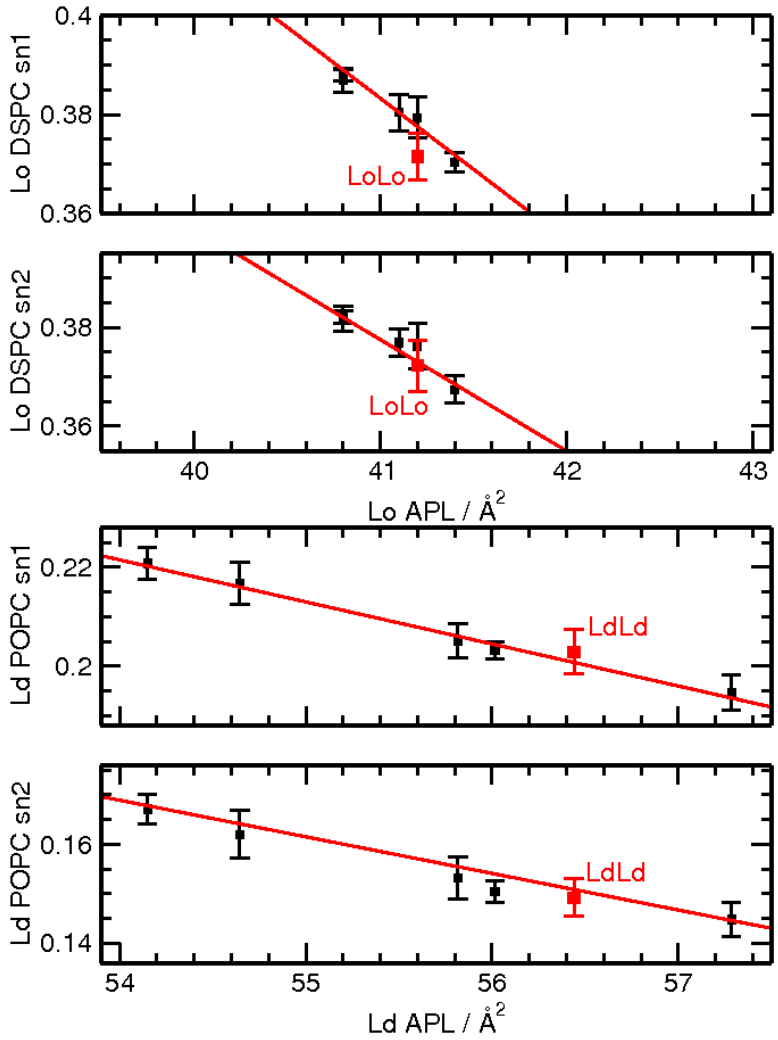

Figure 8. Averaged acyl chain order parameters for the sn-1 and sn-2 chains of DSPC in the Lo phase and the sn-1 and sn-2 chains of POPC in the Ld phase, plotted as a function of APL. Red lines are the least squares fit to the data.

Order parameters Deuterium order parameters averaged over all acyl chain carbons were calculated for each bilayer leaflet, and the results as a function of APL are shown in

Figure 8. Both the DSPC order parameter (in the Lo leaflet) and the POPC order parameter (in the Ld leaflet) decrease almost linearly with increasing APL. The magnitude of the decrease is larger for the Ld phase, but the change of APL is five times greater in the Ld leaflet. Comparing the fits to the data (Figure 8) allows us to roughly quantify the sensitivity of the deuterium order parameter to changes in APL. For example, the slope in the Lo leaflet is three times that of the Ld leaflet, suggesting that the order parameter (acyl chain orientational mobility) in the Lo leaflet is three times more sensitive to the local lipid packing than in the Ld leaflet.

These differences in order parameters point to coupling through a mismatch in the free energy related to the entropic contributions relating chain disorder and APL. From the computed deuterium order parameter S_{CD}, the associated configurational entropy can be estimated using $\Delta S = k_B \ln(3 - (1 + 8S_{CD})^{\frac{1}{2}})$. [70] Adding 20 lipids (an increase of ~6%) to the Ld leaflet of LoLd(-10) bilayers (resulting in LoLd(+10)) causes APL to decrease from 57.3 $Å^2$ to 54.1 $Å^2$ in the Ld leaflet and increase from 40.8 $Å^2$ to 41.4 $Å^2$ in the apposing Lo leaflet. This causes the configurational entropy to change by -0.0924 cal/(mol·K) in the Ld leaflet and 0.0693 cal/(mol·K) in the Lo leaflet. When multiplied by their respective number of lipids per unit area, the entropy decrease of the Ld leaflet is compensated exactly by the entropy increase in the Lo leaflet. If one considers that the order parameter measures the local volume being sampled, the two estimated entropy values are consistent with each other, as the total volume is conserved for each leaflet. However, our model constrained the two leaflets to the same surface area. If this constraint is relaxed – as in the case of a free-floating vesicle studied experimentally –

this entropy compensation diminishes for an asymmetric alignment of the Lo and Ld leaflets, thus providing a mechanism for interleaflet coupling through local density fluctuations. The entropic gain for a registered *vs.* an anti-registered domain of size of 68 Å is estimated to be ~7 kcal/mol at 6% of the local density change at room temperature.

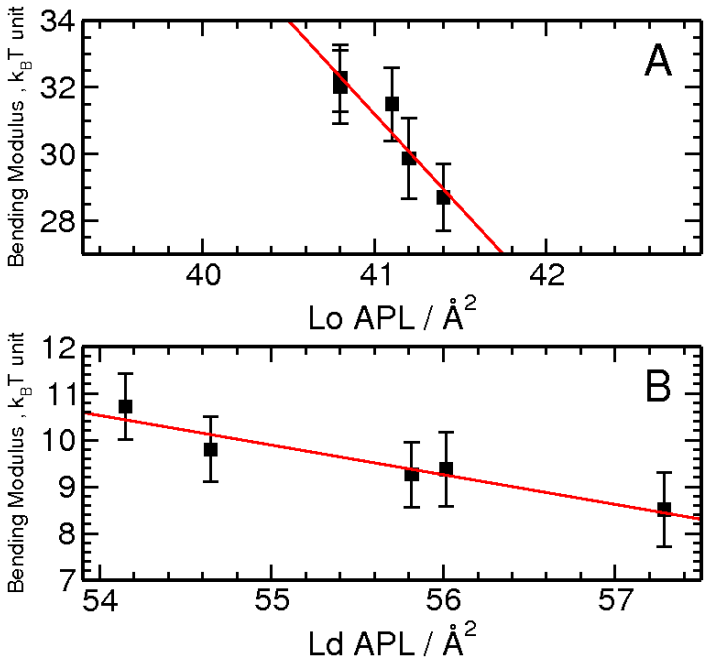

Figure 9. Monolayer bending moduli of (A) Lo and (B) Ld leaflets as a function of APL in the five asymmetric systems studied.

Bending modulus The monolayer bending modulus was calculated following Khelashvili et al. method[71] by evaluating all the pairwise lipid splay angles in the ternary mixture system, and performing a quadratic fit to the potential of the mean force of the splay angle distribution. The bending moduli of individual Ld and Lo leaflets are shown in Figure 9 for the five asymmetric lipid bilayers. Overall, the calculated bending moduli are consistent with those reported previously[43] – considering these values are for a monolayer. As APL increases, the bending modulus decreases linearly, with the largest

value of 10.71±0.7 k_BT at 54.15 Å^2 and the smallest value of 8.51±0.8 k_BT at 57.29 Å^2 for the Ld leaflets. In the case of Lo leaflets, the largest and smallest values, respectively are 32.27±1.0 k_BT at 40.8 Å^2 and 28.69±1.0 k_BT at 41.4 Å^2. The results clearly show that the bending moduli of both leaflets are very sensitive to the lipid packing in the Ld leaflets. Changing from the LoLd(-10) to LoLd(+10) bilayers causes the bending modulus to change by 2.2±1.5 k_BT for the Ld leaflet and -3.58±1.6 k_BT for the Lo leaflet, roughly leading to a compensation of the bending free energy between the two leaflets. This again provides a potential mechanism for interleaflet coupling through local density fluctuations.

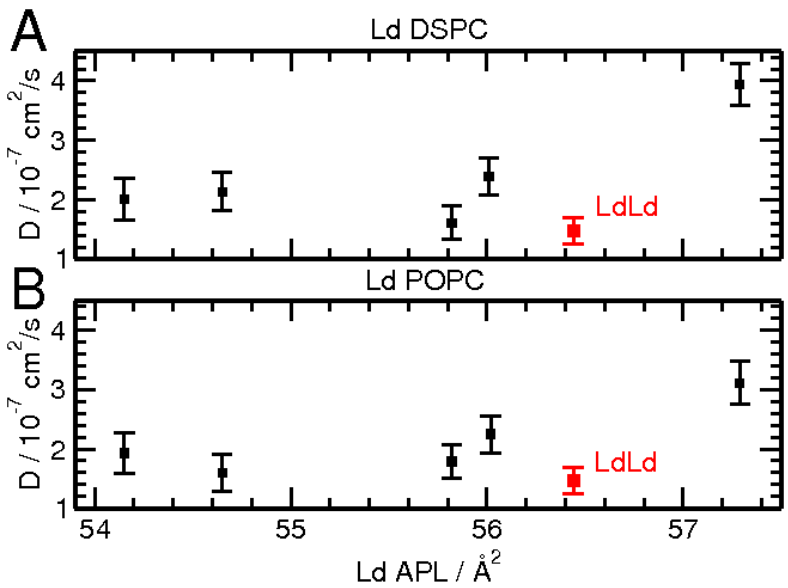

Figure 10. Diffusion coefficients of (A) DSPC and (B) POPC in Ld leaflets as a function of APL.

Lateral diffusion As shown in Figure 10, the self-diffusion coefficients of Ld DSPC and Ld POPC leaflets remain roughly constant as APL increases – exception being the 57.3

Å^2 APL. Compared to leaflet properties such as the order parameter and bending modulus, it is somewhat surprising that the lipid lateral diffusion is relatively insensitive to changes in APL (within 6%). However, we anticipate a statistically significant change in the diffusion coefficient with a greater increase (i.e., >6%) in APL. In fact, the unusually high diffusion coefficient observed for APL = 57.3 Å^2 may indicate that the system has reached a transition point where the lipids are packed loosely enough to alter their diffusion behavior.

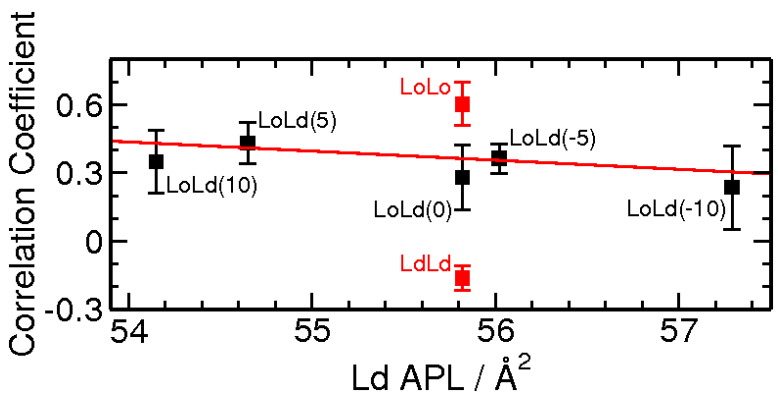

Figure 11. Lipid HGPC coefficient as a function of Ld leaflet APL for the five asymmetric bilayer systems (LoLd(0), LoLd(-5), LoLd(5), LoLd(-10), and LoLd(10)), including the symmetric LoLo and LdLd bilayers.

Lipid head group position correlation (HGPC) across leaflets As shown in Figure 11, HGPC coefficients for the additional four asymmetric bilayer systems are similar to the LoLd(0) system. This agreement suggests that the leaflets in all asymmetric bilayers behave as a single unit. We further fitted the HGPC coefficient data as a function of Ld leaflet APL, and found that HGPC increases as APL decreases. With decreasing APL, the lipids pack more densely, the Ld leaflet becomes less compressible, and HGPC increases.

In this section, we explore the how the different properties of the two apposing leaflets are affected by changes in intraleaflet lipid packing by systematically varying the number of lipids in the Ld leaflets. While no effect on the acyl chain interdigitation is observed in these asymmetric systems, APL, order parameters and bending moduli are all affected by changes in lipid packing. This shows that small changes in lipid packing density, modeled here by adding or removing a small fraction (a few percent) of lipids from one bilayer leaflet, can have a significant effect not only on its own properties, but those of the apposing leaflet, thus providing a mechanism for the interleaflet coupling. For example, curvature/composition fluctuations can modulate the local packing density, thus leading to the apparent cross-layer coupling that has been observed experimentally. Importantly, most structural and mechanical bilayer leaflet properties such as order parameters and bending moduli, show a linear relationship with APL. Changes to the order parameters in the two apposing leaflets are found to be correlated, and compensate each other across bilayer leaflets. These results highlight the direct intraleaflet (packing) effect on leaflet properties, as well as the indirect interleaflet coupling effect arising from the compensatory changes in lipid packing across bilayer leaflets.

Discussion

Domain registration in DSPC/POPC/CHL ternary mixtures has recently been observed by SANS experiments,[43] but the underlying molecular mechanisms remain elusive. In the present study, we have examined acyl chain interdigitation as a potential factor for interleaflet coupling in symmetric and asymmetric non-phase-separated (homogeneous

Lo/Ld phase) lipid bilayers. Acyl chain interdigitation has been implicated as the main factor for interleaflet coupling in studies using phenomenological models,[31] but no detailed molecular-level study has been reported. Our simulations show that the structural and dynamical properties of the individual leaflets of this system are not affected by the phase properties of their apposing leaflets, suggesting that dynamic chain interdigitation is not a necessary mechanism for interleaflet coupling.[28] However, our simulations only implicitly considered laterally homogeneous bilayer models, so we cannot exclude the possibility of strong interdigitation at domain boundaries. Additionally, interdigitation may be a significant factor when dramatic differences exist in the acyl chains (e.g., length, degree of unsaturation, etc.).[58]

Spontaneous curvature and local composition coupling has also been suggested for raft formation and registration.[38, 72-73] In our systems, the Lo and Ld phases are composed of the same lipids, but with different molar ratios. The spontaneous curvature parameters for DSPC, POPC and CHL are -0.1000 ± 0.044, -0.022 ± 0.010, and -0.494 ± 0.013 nm^{-1}, respectively.[74] Assuming full miscibility and linear additivity, we obtain spontaneous curvatures for the Ld and Lo phases to be -0.103 and -0.183 nm^{-1}, respectively, which means that the Lo phase has a stronger tendency to bend than the Ld phase. These numbers agree qualitatively with the results obtained by Nickels et al.[43] However, our simulations appear insensitive to spontaneous curvature on the interleaflet coupling (by visual examination of the trajectories), because a much larger bilayer system is needed to observe this effect.

Similarly, other possible factors contributing to interleaflet coupling, such as electrostatic coupling,[31] cholesterol flip-flop,[75] coupling of transmembrane proteins,[76] overhang energy penalty,[28] line tension[42] and curvature,[67] may be better investigated in models where the minimization of interfacial energy and line tension are can be directly considered as potential mechanisms. Heberle et al. performed contrast-matched neutron scattering experiments on lipid vesicles, and suggested that bilayer thickness mismatch controls raft size. This result was related to the role of line tension in raft formation using the theory of Kuzmin.[42 77]

Interleaflet domain coupling (raft registration/anti-registration) is likely the result of the balance between several competing mechanisms.[37, 77] To account for line tension, it would require transversally asymmetric and laterally non-homogeneous bilayer models (with mixed Lo and Ld phases in the same leaflet) to be studied; all atom simulations of such bilayer systems are currently ongoing. Nevertheless, the present studies of non-phase-separated asymmetric systems show that dynamic chain interdigitation is weak, consistent with observations in supported lipid bilayer studies.[78]Our simulation results highlight that of the leaflet properties studied, deuterium order parameters and bending moduli are affected by intraleaflet lipid packing. This interplay between the local lipid density and bending modulus may play a role in governing interleaflet domain coupling in lipid bilayers.

Conclusion

We have performed MD simulations of symmetric and asymmetric Lo/Ld lipid bilayers composed of POPC/DSPC/CHL to study interleaflet coupling. By constructing an asymmetric bilayer from leaflets taken from equilibrated symmetric bilayers, we found little interleaflet coupling between apposing bilayer leaflets, i.e., the properties of the individual leaflets remain the same as those in the corresponding symmetric bilayers. These results thus suggest that acyl chain interdigitation is not an important factor for interleaflet coupling for this nanodomain forming lipid composition. When systematically adding or removing lipids in one of the leaflets, we observed strong intra- and inter-leaflet coupling effects on APL, deuterium order parameters, and bending moduli, suggesting that the leaflet properties are extremely sensitive to lipid packing. We also showed that the interplay between acyl chain dynamics and bending moduli in the two leaflets could potentially contribute to interleaflet coupling. Collectively, our simulations suggest that acyl chain interdigitation alone does not contribute to interleaflet coupling, but local lipid packing fluctuations, and the resultant changes in the bilayers elastic properties, can provide a plausible mechanism for interleaflet coupling in biological membrane systems.

Supporting Information Available

Supporting materials contain information of mean square displacement of DSPC and POPC lipids in the Ld leaflet of LoLd(0) compared to the LdLd symmetric system are available at http://pubs.acs.org/journal/jpcbfk.

Acknowledgement

JT and XC are partially supported by the Laboratory Directed R&D (LDRD) Fund at the Oak Ridge National Laboratory. JK is supported through the Scientific User Facilities

Division of the DOE Office of Basic Energy Sciences (BES), under contract no. DE-AC05 00OR2275. This research used resources of the Oak Ridge Leadership Computing Facility at the Oak Ridge National Laboratory, which is supported by the Office of Science of the U.S. Department of Energy under Contract No. DE-AC05-00OR22725.

References

1. Singer, S. J.; Nicolson, G. L. The fluid mosaic model of the structure of cell membranes. *Science (New York, N.Y.)* **1972,** *175* (4023), 720-31.
2. Bretscher, M. S. Asymmetrical lipid bilayer structure for biological membranes. *Nature* **1972,** *236* (61), 11-12.
3. van Meer, G. Dynamic transbilayer lipid asymmetry. *Cold Spring Harbor perspectives in biology* **2011,** *3* (5), a004671.
4. Simons, K.; Ikonen, E. Functional rafts in cell membranes. *Nature* **1997,** *387* (6633), 569-72.
5. Simons, K.; Toomre, D. Lipid rafts and signal transduction. *Nature reviews Molecular cell biology* **2000,** *1* (1), 31-39.
6. Gajate, C.; Mollinedo, F. The antitumor ether lipid ET-18-OCH3 induces apoptosis through translocation and capping of Fas/CD95 into membrane rafts in human leukemic cells. *Blood* **2001,** *98* (13), 3860-3863.
7. del Pozo, M. A.; Alderson, N. B.; Kiosses, W. B.; Chiang, H.-H.; Anderson, R. G.; Schwartz, M. A. Integrins regulate Rac targeting by internalization of membrane domains. *Science (New York, N.Y.)* **2004,** *303* (5659), 839-842.
8. Pierce, S. K. Lipid rafts and B-cell activation. *Nature Reviews Immunology* **2002,** *2* (2), 96-105.
9. Hering, H.; Lin, C.-C.; Sheng, M. Lipid rafts in the maintenance of synapses, dendritic spines, and surface AMPA receptor stability. *The Journal of neuroscience* **2003,** *23* (8), 3262-3271.
10. Villalba, M.; Bi, K.; Rodriguez, F.; Tanaka, Y.; Schoenberger, S.; Altman, A. Vav1/Rac-dependent actin cytoskeleton reorganization is required for lipid raft clustering in T cells. *The Journal of cell biology* **2001,** *155* (3), 331-338.
11. Lingwood D; Simons K. Lipid rafts as a membrane-organizing principle. *Science (New York, N.Y.)* **2010,** *327* (5961), 46-50.
12. Jacobson K; Mouritsen OG; Anderson RG. Lipid rafts: at a crossroad between cell biology and physics. *Nat Cell Biol* **2007,** *9* (1), 7-14.
13. Fadok, V. A.; Voelker, D. R.; Campbell, P. A.; Cohen, J. J.; Bratton, D. L.; Henson, P. M. Exposure of phosphatidylserine on the surface of apoptotic lymphocytes triggers specific recognition and removal by macrophages. *The Journal of Immunology* **1992,** *148* (7), 2207-2216.

14. Martin, S.; Reutelingsperger, C.; McGahon, A. J.; Rader, J. A.; Van Schie, R.; LaFace, D. M.; Green, D. R. Early redistribution of plasma membrane phosphatidylserine is a general feature of apoptosis regardless of the initiating stimulus: inhibition by overexpression of Bcl-2 and Abl. *The Journal of experimental medicine* **1995,** *182* (5), 1545-1556.
15. Bennett, M.; Gibson, D.; Schwartz, S.; Tait, J. Binding and phagocytosis of apoptotic vascular smooth muscle cells is mediated in part by exposure of phosphatidylserine. *Circulation research* **1995,** *77* (6), 1136-1142.
16. Casciola-Rosen, L.; Rosen, A.; Petri, M.; Schlissel, M. Surface blebs on apoptotic cells are sites of enhanced procoagulant activity: implications for coagulation events and antigenic spread in systemic lupus erythematosus. *Proceedings of the National Academy of Sciences* **1996,** *93* (4), 1624-1629.
17. Zwaal, R. F. A.; Comfurius, P.; Van Deenen, L. L. M. Membrane asymmetry and blood coagulation. *Nature* **1977,** *268* (5618), 358-360.
18. Bevers, E. M.; Comfurius, P.; Vanrijn, J.; Hemker, H. C.; Zwaal, R. F. A. Generation of prothrombin-converting activity and the exposure of phosphatidylserine at the outer surface of platelets. *Eur. J. Biochem.* **1982,** *122* (2), 429-436.
19. Tanaka, Y.; Schroit, A. Insertion of fluorescent phosphatidylserine into the plasma membrane of red blood cells. Recognition by autologous macrophages. *Journal of Biological Chemistry* **1983,** *258* (18), 11335-11343.
20. Schroit, A. J.; Madsen, J. W.; Tanaka, Y. In vivo recognition and clearance of red blood cells containing phosphatidylserine in their plasma membranes. *Journal of Biological Chemistry* **1985,** *260* (8), 5131-5138.
21. Fadok, V. A.; Laszlo, D. J.; Noble, P. W.; Weinstein, L.; Riches, D.; Henson, P. Particle digestibility is required for induction of the phosphatidylserine recognition mechanism used by murine macrophages to phagocytose apoptotic cells. *The Journal of Immunology* **1993,** *151* (8), 4274-4285.
22. Connor, J.; Bucana, C.; Fidler, I. J.; Schroit, A. J. Differentiation-dependent expression of phosphatidylserine in mammalian plasma membranes: quantitative assessment of outer-leaflet lipid by prothrombinase complex formation. *Proceedings of the National Academy of Sciences* **1989,** *86* (9), 3184-3188.
23. Utsugi, T.; Schroit, A. J.; Connor, J.; Bucana, C. D.; Fidler, I. J. Elevated expression of phosphatidylserine in the outer membrane leaflet of human tumor cells and recognition by activated human blood monocytes. *Cancer Research* **1991,** *51* (11), 3062-3066.
24. Pike, L. J. Rafts defined: a report on the Keystone Symposium on Lipid Rafts and Cell Function. *Journal of lipid research* **2006,** *47* (7), 1597-8.
25. Marsh, D. Cholesterol-induced fluid membrane domains: A compendium of lipid-raft ternary phase diagrams. *Biochimica et Biophysica Acta (BBA) - Biomembranes* **2009,** *1788* (10), 2114-2123.
26. Elson, E. L.; Fried, E.; Dolbow, J. E.; Genin, G. M. Phase separation in biological membranes: integration of theory and experiment. *Annual review of biophysics* **2010,** *39*, 207-26.

27. Wang, T. Y.; Silvius, J. R. Cholesterol does not induce segregation of liquid-ordered domains in bilayers modeling the inner leaflet of the plasma membrane. *Biophysical journal* **2001,** *81* (5), 2762-73.
28. Collins, M. D.; Keller, S. L. Tuning lipid mixtures to induce or suppress domain formation across leaflets of unsupported asymmetric bilayers. *Proceedings of the National Academy of Sciences of the United States of America* **2008,** *105* (1), 124-8.
29. Nickels, J. D.; Smith, J. C.; Cheng, X. Lateral Organization, Bilayer Asymmetry, and Inter-Leaflet Coupling of Biological Membranes. *Chemistry and Physics of Lipids* **2015,** *192*, 87-99.
30. Almeida, P. F. F. Thermodynamics of lipid interactions in complex bilayers. *Biochimica et Biophysica Acta (BBA) - Biomembranes* **2009,** *1788* (1), 72-85.
31. May, S. Trans-monolayer coupling of fluid domains in lipid bilayers. *Soft matter* **2009,** *5* (17), 3148.
32. Turner, M. S.; Sens, P.; Socci, N. D. Nonequilibrium raftlike membrane domains under continuous recycling. *Physical review letters* **2005,** *95* (16), 168301.
33. Chiantia, S.; London, E. Acyl chain length and saturation modulate interleaflet coupling in asymmetric bilayers: effects on dynamics and structural order. *Biophysical journal* **2012,** *103* (11), 2311-9.
34. Feigenson, G. W. Phase diagrams and lipid domains in multicomponent lipid bilayer mixtures. *Biochimica et Biophysica Acta (BBA) - Biomembranes* **2009,** *1788* (1), 47-52.
35. Devaux, P. F.; Morris, R. Transmembrane asymmetry and lateral domains in biological membranes. *Traffic (Copenhagen, Denmark)* **2004,** *5* (4), 241-6.
36. Perlmutter, J. D.; Sachs, J. N. Interleaflet interaction and asymmetry in phase separated lipid bilayers: molecular dynamics simulations. *Journal of the American Chemical Society* **2011,** *133* (17), 6563-77.
37. Collins, M. D. Interleaflet coupling mechanisms in bilayers of lipids and cholesterol. *Biophysical journal* **2008,** *94* (5), L32-4.
38. Meinhardt, S.; Vink, R. L.; Schmid, F. Monolayer curvature stabilizes nanoscale raft domains in mixed lipid bilayers. *Proceedings of the National Academy of Sciences of the United States of America* **2013,** *110* (12), 4476-81.
39. Shlomovitz, R.; Schick, M. Model of a raft in both leaves of an asymmetric lipid bilayer. *Biophysical journal* **2013,** *105* (6), 1406-13.
40. Amazon, J. J.; Goh, S. L.; Feigenson, G. W. Competition between line tension and curvature stabilizes modulated phase patterns on the surface of giant unilamellar vesicles: a simulation study. *Physical Review E* **2013,** *87* (2), 022708.
41. Seul, M.; Andelman, D. Domain shapes and patterns: the phenomenology of modulated phases. *Science (New York, N.Y.)* **1995,** *267* (5197), 476-483.
42. Heberle, F. A.; Petruzielo, R. S.; Pan, J.; Drazba, P.; Kucerka, N.; Standaert, R. F.; Feigenson, G. W.; Katsaras, J. Bilayer thickness mismatch controls domain size in model membranes. *Journal of the American Chemical Society* **2013,** *135* (18), 6853-9.
43. Nickels, J. D.; Cheng, X.; Mostofian, B.; Stanley, C.; Lindner, B.; Heberle, F. A.; Perticaroli, S.; Feygenson, M.; Egami, T.; Standaert, R. F.; Smith, J. C.; Myles, D. A.; Ohl, M.; Katsaras, J. Mechanical Properties of Nanoscopic Lipid Domains. *Journal of the American Chemical Society* **2015**.

44. Konyakhina, T. M.; Goh, S. L.; Amazon, J.; Heberle, F. A.; Wu, J.; Feigenson, G. W. Control of a nanoscopic-to-macroscopic transition: modulated phases in four-component DSPC/DOPC/POPC/Chol giant unilamellar vesicles. *Biophysical journal* **2011,** *101* (2), L8-L10.
45. Fitter, J.; Lechner, R.; Dencher, N. Interactions of hydration water and biological membranes studied by neutron scattering. *The Journal of Physical Chemistry B* **1999,** *103* (38), 8036-8050.
46. Pronk, S.; Pall, S.; Schulz, R.; Larsson, P.; Bjelkmar, P.; Apostolov, R.; Shirts, M. R.; Smith, J. C.; Kasson, P. M.; van der Spoel, D.; Hess, B.; Lindahl, E. GROMACS 4.5: a high-throughput and highly parallel open source molecular simulation toolkit. *Bioinformatics (Oxford, England)* **2013,** *29* (7), 845-54.
47. Klauda, J. B.; Venable, R. M.; Freites, J. A.; O'Connor, J. W.; Tobias, D. J.; Mondragon-Ramirez, C.; Vorobyov, I.; MacKerell, A. D., Jr.; Pastor, R. W. Update of the CHARMM all-atom additive force field for lipids: validation on six lipid types. *The journal of physical chemistry. B* **2010,** *114* (23), 7830-43.
48. Jorgensen, W. L.; Chandrasekhar, J.; Madura, J. D.; Impey, R. W.; Klein, M. L. Comparison of simple potential functions for simulating liquid water. *The Journal of chemical physics* **1983,** *79* (2), 926-935.
49. Hoover, W. G. Canonical dynamics: Equilibrium phase-space distributions. *Physical review. A* **1985,** *31* (3), 1695-1697.
50. Nose, S. A MOLECULAR-DYNAMICS METHOD FOR SIMULATIONS IN THE CANONICAL ENSEMBLE. *Molecular Physics* **1984,** *52* (2), 255-268.
51. Parrinello, M.; Rahman, A. POLYMORPHIC TRANSITIONS IN SINGLE-CRYSTALS - A NEW MOLECULAR-DYNAMICS METHOD. *Journal of Applied Physics* **1981,** *52* (12), 7182-7190.
52. Essmann, U.; Perera, L.; Berkowitz, M. L.; Darden, T.; Lee, H.; Pedersen, L. G. A SMOOTH PARTICLE MESH EWALD METHOD. *Journal of Chemical Physics* **1995,** *103* (19), 8577-8593.
53. Piggot, T. J.; Pineiro, A.; Khalid, S. Molecular Dynamics Simulations of Phosphatidylcholine Membranes: A Comparative Force Field Study. *Journal of chemical theory and computation* **2012,** *8* (11), 4593-609.
54. Miyamoto, S.; Kollman, P. A. SETTLE - AN ANALYTICAL VERSION OF THE SHAKE AND RATTLE ALGORITHM FOR RIGID WATER MODELS. *Journal of Computational Chemistry* **1992,** *13* (8), 952-962.
55. Hess, B.; Bekker, H.; Berendsen, H. J. C.; Fraaije, J. LINCS: A linear constraint solver for molecular simulations. *Journal of Computational Chemistry* **1997,** *18* (12), 1463-1472.
56. Vanegas, J. M.; Torres-Sanchez, A.; Arroyo, M. Importance of Force Decomposition for Local Stress Calculations in Biomembrane Molecular Simulations. *Journal of chemical theory and computation* **2014,** *10* (2), 691-702.
57. Capponi, S.; Freites, J. A.; Tobias, D. J.; White, S. H. Interleaflet mixing and coupling in liquid-disordered phospholipid bilayers. *Biochimica et biophysica acta* **2016,** *1858* (2), 354-62.
58. Niemela, P. S.; Hyvonen, M. T.; Vattulainen, I. Influence of chain length and unsaturation on sphingomyelin bilayers. *Biophysical journal* **2006,** *90* (3), 851-63.

59. Marrink, S. J.; Risselada, H. J.; Yefimov, S.; Tieleman, D. P.; de Vries, A. H. The MARTINI Force Field: Coarse Grained Model for Biomolecular Simulations. *The Journal of Physical Chemistry B* **2007,** *111* (27), 7812-7824.
60. Klauda, J. B.; Brooks, B. R.; Pastor, R. W. Dynamical motions of lipids and a finite size effect in simulations of bilayers. *The Journal of chemical physics* **2006,** *125* (14), 144710.
61. Almeida, P. F.; Vaz, W. L.; Thompson, T. E. Lipid diffusion, free area, and molecular dynamics simulations. *Biophysical journal* **2005,** *88* (6), 4434-8.
62. Falck, E.; Patra, M.; Karttunen, M.; Hyvonen, M. T.; Vattulainen, I. Lessons of slicing membranes: interplay of packing, free area, and lateral diffusion in phospholipid/cholesterol bilayers. *Biophysical journal* **2004,** *87* (2), 1076-91.
63. Oradd, G.; Westerman, P. W.; Lindblom, G. Lateral diffusion coefficients of separate lipid species in a ternary raft-forming bilayer: a Pfg-NMR multinuclear study. *Biophysical journal* **2005,** *89* (1), 315-20.
64. Wohlert, J.; Edholm, O. Dynamics in atomistic simulations of phospholipid membranes: Nuclear magnetic resonance relaxation rates and lateral diffusion. *The Journal of chemical physics* **2006,** *125* (20), 204703.
65. Skjevik, A. A.; Madej, B. D.; Dickson, C. J.; Teigen, K.; Walker, R. C.; Gould, I. R. All-atom lipid bilayer self-assembly with the AMBER and CHARMM lipid force fields. *Chemical communications* **2015,** *51* (21), 4402-5.
66. Galimzyanov, T. R.; Molotkovsky, R. J.; Bozdaganyan, M. E.; Cohen, F. S.; Pohl, P.; Akimov, S. A. Elastic Membrane Deformations Govern Interleaflet Coupling of Lipid-Ordered Domains. *Physical review letters* **2015,** *115* (8), 088101.
67. Pantano, D. A.; Moore, P. B.; Klein, M. L.; Discher, D. E. Raft registration across bilayers in a molecularly detailed model. *Soft matter* **2011,** *7* (18), 8182.
68. Lin, W. C.; Blanchette, C. D.; Ratto, T. V.; Longo, M. L. Lipid asymmetry in DLPC/DSPC-supported lipid bilayers: a combined AFM and fluorescence microscopy study. *Biophysical journal* **2006,** *90* (1), 228-37.
69. Bhide, S. Y.; Zhang, Z.; Berkowitz, M. L. Molecular dynamics simulations of SOPS and sphingomyelin bilayers containing cholesterol. *Biophysical journal* **2007,** *92* (4), 1284-95.
70. Yang, D.; Kay, L. E. Contributions to conformational entropy arising from bond vector fluctuations measured from NMR-derived order parameters: application to protein folding. *Journal of molecular biology* **1996,** *263* (2), 369-82.
71. Khelashvili, G.; Kollmitzer, B.; Heftberger, P.; Pabst, G.; Harries, D. Calculating the Bending Modulus for Multicomponent Lipid Membranes in Different Thermodynamic Phases. *Journal of chemical theory and computation* **2013,** *9* (9), 3866-3871.
72. Sadeghi, S.; Muller, M.; Vink, R. L. Raft formation in lipid bilayers coupled to curvature. *Biophysical journal* **2014,** *107* (7), 1591-600.
73. Parthasarathy, R.; Groves, J. T. Curvature and spatial organization in biological membranes. *Soft matter* **2007,** *3* (1), 24-33.
74. Kollmitzer, B.; Heftberger, P.; Rappolt, M.; Pabst, G. Monolayer spontaneous curvature of raft-forming membrane lipids. *Soft matter* **2013,** *9* (45), 10877-10884.
75. Kornberg, R. D.; McConnell, H. M. Inside-outside transitions of phospholipids in vesicle membranes. *Biochemistry* **1971,** *10* (7), 1111-20.

76. Lingwood, D.; Ries, J.; Schwille, P.; Simons, K. Plasma membranes are poised for activation of raft phase coalescence at physiological temperature. *Proceedings of the National Academy of Sciences of the United States of America* **2008,** *105* (29), 10005-10.
77. Kuzmin, P. I.; Akimov, S. A.; Chizmadzhev, Y. A.; Zimmerberg, J.; Cohen, F. S. Line tension and interaction energies of membrane rafts calculated from lipid splay and tilt. *Biophysical journal* **2005,** *88* (2), 1120-33.
78. Alessandrini, A.; Facci, P. Model Bio-Membranes Investigated by AFM and AFS: A Suitable Tool to Unravel Lipid Organization and their Interactions with Proteins. *Smart Membrane Sensors, Scrivener Publishing LLC* **2014**, 185-226.
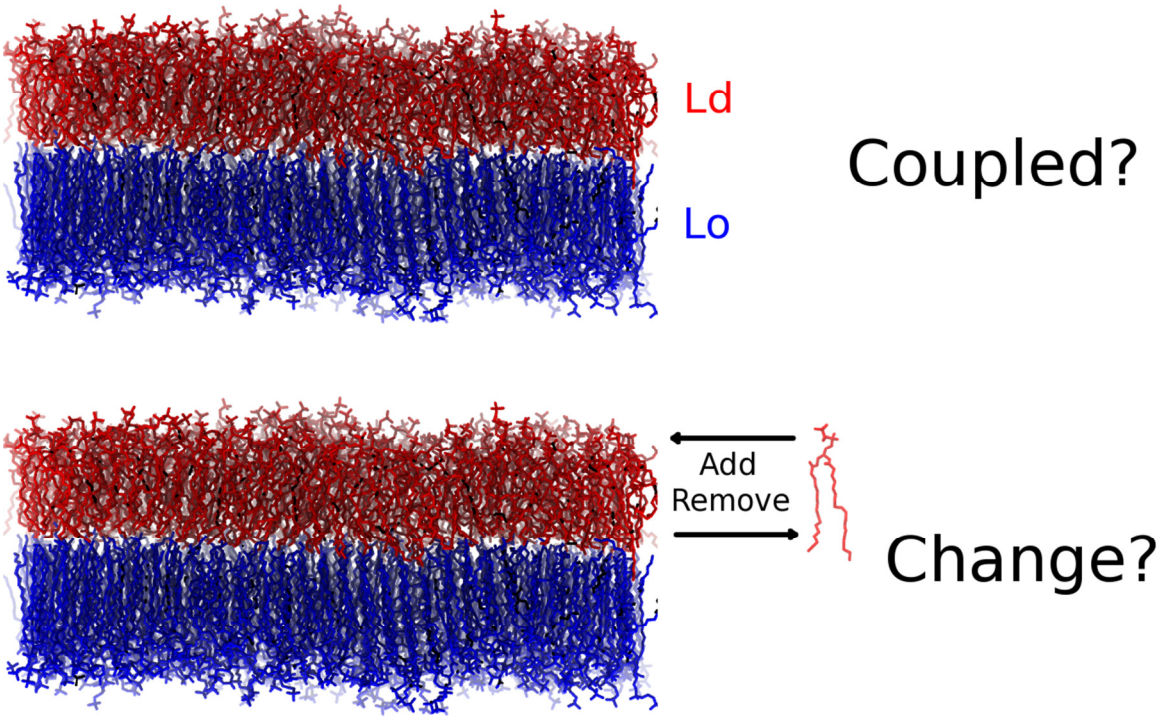
TOC image